Chemical Physics 373 (2010) 203–210

Contents lists available at ScienceDirect

Chemical Physics

journal homepage: www.elsevier.com/locate/chemphys

Empirical line parameters of methane in the 1.63–1.48 μm transparency window by high sensitivity Cavity Ring Down Spectroscopy

A. Campargue [a,*], L. Wang [a], A.W. Liu [a,b], S.M. Hu [b], S. Kassi [a]

[a] Laboratoire de Spectrométrie Physique (Associated with CNRS, UMR 5588), Université Joseph Fourier de Grenoble, B.P. 87, 38402 Saint-Martin-d'Hères Cedex, France
[b] Hefei National Laboratory for Physical Sciences at Microscale, University of Science and Technology of China, Hefei 230026, China

ARTICLE INFO

Article history:
Received 4 April 2010
In final form 10 May 2010
Available online 31 May 2010

Keywords:
Methane
CH_4
CH_3D
Titan
CRDS
HITRAN

ABSTRACT

The positions and intensities of methane in the 1.58 μm transparency window have been measured by high sensitivity Cavity Ring Down Spectroscopy at room temperature. The achieved sensitivity allowed measuring intensities as small as 3×10^{-29} cm/molecule i.e. three orders of magnitude smaller than the intensity cut off of the HITRAN line list of methane. The complete list contains a total of 16,149 transitions between 6165 and 6750 cm^{-1}. Their intensity values vary over six orders of magnitude from 1.6×10^{-29} to 2.5×10^{-23} cm/molecule. Transitions due to CH_3D in "natural" abundance in our methane sample were identified using a new spectrum of CH_3D recorded separately with a Fourier Transform spectrometer. From simulations of the CH_3D and methane spectra at low resolution, the CH_3D isotopologue has be found to contribute by up to 30% of the absorption near 1.58 μm.

1. Introduction

Methane is present in a large variety of astronomical objects including Titan, giant outer planets and comets. In view of applications to planetary science, the knowledge of the absorption spectrum of methane at very high sensitivity is required in particular in the spectral windows of low opacity. While the $^{12}CH_4$ infrared absorption spectrum can be theoretically modelled above 2 μm, the near infrared spectrum is not yet understood and lists of empirical line parameters provide an alternative solution. The difficulties encountered in the theoretical treatment are a consequence of the extreme spectral congestion in the near infrared region caused by anharmonic couplings between stretching and bending modes that leads to complicated polyad structure [1]. Due to approximate relations between the vibrational frequencies, $\nu_1 \approx \nu_3 \approx 2\nu_2 \approx 2\nu_4$, each polyad is characterized by a polyad number $P = 2(V_1 + V_3) + V_2 + V_4$, where V_i are the normal mode vibrational quantum numbers. The present report is devoted to the 1.63–1.48 μm transparency window lying between the tetradecad ($P = 4$) region dominated by the $2\nu_3$ band at 6004 cm^{-1} and the icosad ($P = 5$) region. Theoretical calculations (see Ref. [2] for instance) show that the lowest bands of the icosad which are very weak (in particular $5\nu_4$) fall in our region and are then partly responsible of the residual absorption. Due to the high density of states in interaction – the icosad contains 20 vibrational levels and 134 sub-levels [1] – standard iterative techniques of spectral analysis cannot be applied because no regular rotational progressions can be identified even for the lowest rotational states. In consequence, above 5000 cm^{-1} the HITRAN08 database [3] provides empirical line by line spectroscopic parameters without rovibrational assignments. The upper panel of Fig. 1 shows the HITRAN line list between 5800 and 7000 cm^{-1}. In the tetradecad region (5500–6150 cm^{-1}), the HITRAN database in its last version [3] reproduces the empirical line positions and intensities obtained by Margolis 20 years ago [4,5]. Note that in HITRAN08, some of the Margolis intensities [4,5] of the $2\nu_3$ transitions were slightly changed using the results obtained by Frankenberg et al. [6]. Above 6180 cm^{-1}, the spectroscopic parameters obtained by Brown by Fourier Transform Spectroscopy (FTS) with path lengths up to 97 m [7] were adopted. As illustrated in Fig. 1, the intensity cut off in the tetradecad region is relatively high (about 4×10^{-24} cm/molecule) i.e. two orders of magnitude higher than above 6180 cm^{-1}. The characterization of the tetradecad has been recently improved by a line list constructed in relation with the "Greenhouse Gases Observing Satellite" (GOSAT) project [8]. The GOSAT line list [9], also presented in Fig. 1, has a 4×10^{-26} cm/molecule intensity cut off which is equivalent to the HITRAN intensity cut off above 6180 cm^{-1}.

The HITRAN08 line list for methane includes also the $3\nu_2$ band of CH_3D of importance for planetary applications (see Fig. 1). The line positions and line intensities were obtained by Lutz et al. [10] and Boussin et al. [11], respectively, from FTS spectra of a CH_3D sample with a sample purity of 96.8%. The HITRAN line intensities being scaled according to the relative abundance of CH_3D in methane (6.15×10^{-4} [3]), it leads to intensity values ranging

* Corresponding author. Tel.: +33 4 76 51 43 19.
E-mail address: Alain.Campargue@ujf-grenoble.fr (A. Campargue).

0301-0104/$ - see front matter © 2010 Elsevier B.V. All rights reserved.
doi:10.1016/j.chemphys.2010.05.011

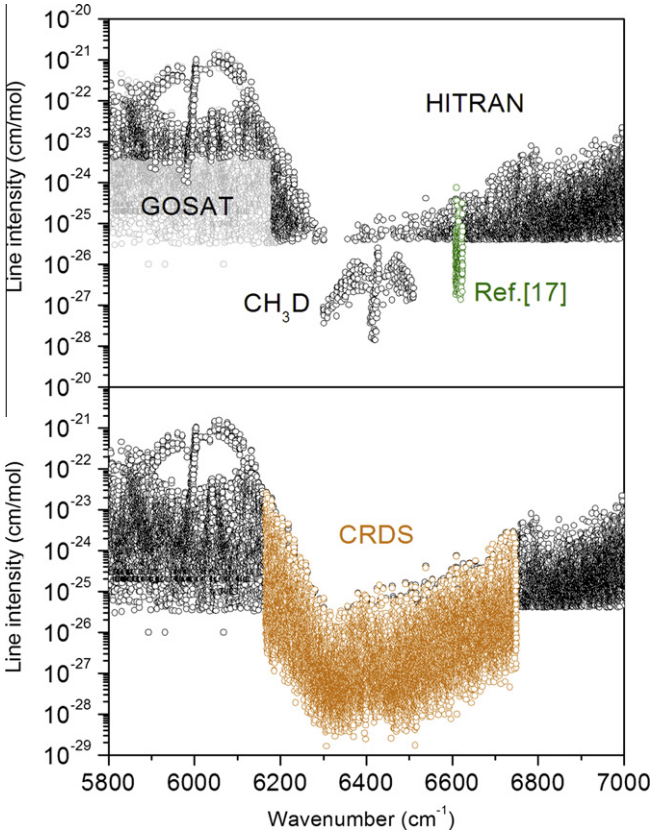

Fig. 1. Overview spectrum of methane at 296 K in the 5800–7000 cm^{-1} region. Upper panel: HITRAN database including the $3\nu_2$ band of CH_3D near 6430 cm^{-1}. The recent GOSAT line list [9] below 6200 cm^{-1} and the results of Ref. [17] in the 6607–6625 cm^{-1} section are also presented. Lower panel: the CRDS line list for the 6165–6750 cm^{-1} region are superimposed on the HITRAN and GOSAT line lists.

between 1.4×10^{-28} and 2.5×10^{-26} cm/molecule i.e. much below the 4×10^{-26} cm/molecule intensity cut off corresponding to the main isotopologue. This CH_3D band at 6430 cm^{-1} has been used to determine the D/H ratio on Titan for instance [12,13]. The CH_3D absorption is then observed superimposed to the absorption of the main isotopologue which is poorly characterized. This is the reason why the analysis of the planetary atmospheres [12–15] used Saturn spectrum as an intermediary spectrum of methane. In a very recent contribution [16], the Cavity Ring Down Spectroscopy technique was used to characterize at high sensitivity the methane absorption spectrum in the region of this $3\nu_2$ band of CH_3D (6289–6526 cm^{-1}). This technique allows increasing by more than 3 orders of magnitude the sensitivity achieved in the FTS measurements [4,5,7,9] used to construct the HITRAN line list. In Ref. [16], the CRDS spectra at room temperature and 79 K were used to derive the lower energy values of the transitions from the variation of their line intensities. The present contribution is devoted to the completion of the spectral coverage of the 6165–6750 cm^{-1} transparency window at room temperature. The lower and upper frequency limits of the investigated region were fixed in such a way that they correspond to relatively strong absorption regions where the additional lines detected by CRDS have a negligible impact compared to the lines previously measured by FTS [4,5,7,9].

As a summary of the results presented below, the lower panel of Fig. 1 shows the overview of the CRDS line list. Including the 6868 transitions measured in Ref. [16], our complete list contains 16,149 lines for the whole 6165–6750 cm^{-1} region. This number should be compared to a total of 1875 CH_4 transitions and 251 CH_3D transitions provided by HITRAN in the same region [3].

In order to complete the review of the previous observations in our region of interest, the results obtained by Deng et al. [17] in the 6607–6625 cm^{-1} section should be mentioned. These authors used direct absorption with a tunable diode laser and a White cell with a 973 m path length to detect 288 lines with intensities down to 1.4×10^{-27} cm/molecule (see Fig. 1upper panel).

The rest of this report is organized as follows: after a brief description of the CW-CRDS spectrometer, we will present in Section 2 the line list construction which was a laborious task considering the congestion and blending of the spectrum. In Section 3, we will compare our line parameters to those provided in the HITRAN database. Section 4 will be devoted to the identification of the CH_3D lines by comparison with a spectrum of CH_3D recorded separately by Fourier Transform Spectroscopy and to the estimation of the importance of the CH_3D contribution from low resolution simulations.

2. Experiment and line list construction

Some of the presently analyzed spectra are those recorded in Ref. [18] but additional recordings were performed extending the spectral coverage and the pressure conditions. The CW-CRDS spectra were obtained with our "standard" fibered DFB laser CW-CRDS spectrometer described in Refs. [18–20]. The 6165.7–6749.5 cm^{-1} region was continuously covered with the help of 27 fibered DFB lasers. The DFB typical tuning range is about 35 cm^{-1} by temperature variation from −5 to 60 °C. The stainless steel ringdown cell (l = 1.42 m, Φ = 10 mm) is fitted by a pair of super mirrors with a typical ring down time on the order of $\tau \sim 60$ μs. About 100 ringdown events were averaged for each spectral data point and 70 min were needed to complete a temperature scan of one DFB laser. The corresponding noise equivalent absorption is on the order of 5×10^{-10} cm^{-1} [18].

The methane sample was purchased from Air Liquide (stated purity >99.995%). During the recordings, the pressure measured by a capacitance gauge and the ringdown cell temperature were monitored. The temperature value was 297 ± 2 K. Most of the spectra were recorded at 2.5 and 10.0 Torr but lower values down to 0.25 Torr were used near the borders of the investigated region where absorption is stronger.

Each 35 cm^{-1} wide spectrum recorded with one DFB laser was calibrated independently on the basis of the wavelength values provided by the Michelson-type wavemeter (Burleigh WA-1650, 60 MHz resolution and 100 MHz accuracy). The wavemeter accuracy being limited to 3×10^{-3} cm^{-1}, the absolute calibration was obtained by a statistical matching of the line positions to those listed in the HITRAN database [3]. Very recently, a high sensitivity FTS spectrum was recorded in Reims (non-apodized resolution of 0.0017 cm^{-1}, l = 1603 m, P = 1 and 5 Torr) [21]. The Reims spectrum could be accurately calibrated against the 30012–00001 band of $^{12}CO_2$ (added in small quantity) near 6348 cm^{-1} [3] which appears superimposed to the methane spectrum. We decided to use this calibrated spectrum to refine the calibration of the CRDS spectra. The comparison with the HITRAN line positions shows a systematic shift of 1.1×10^{-3} cm^{-1} on average compared to Reims spectra, Reims values (and then our values) being larger than HITRAN values. The use of Reims spectrum instead of HITRAN data has also the advantage to solve a significant shift between Margolis [4,5] and Brown [7] calibrations around 6180 cm^{-1}. The precision of the obtained wavenumber calibration estimated from the dispersion of the wavenumber differences is on the order of 1×10^{-3} cm^{-1}.

The overview of the CW-CRDS spectra over the whole transparency window is shown in the upper panel of Fig. 2. Four successive enlargements illustrate the high dynamics on the intensity scale of

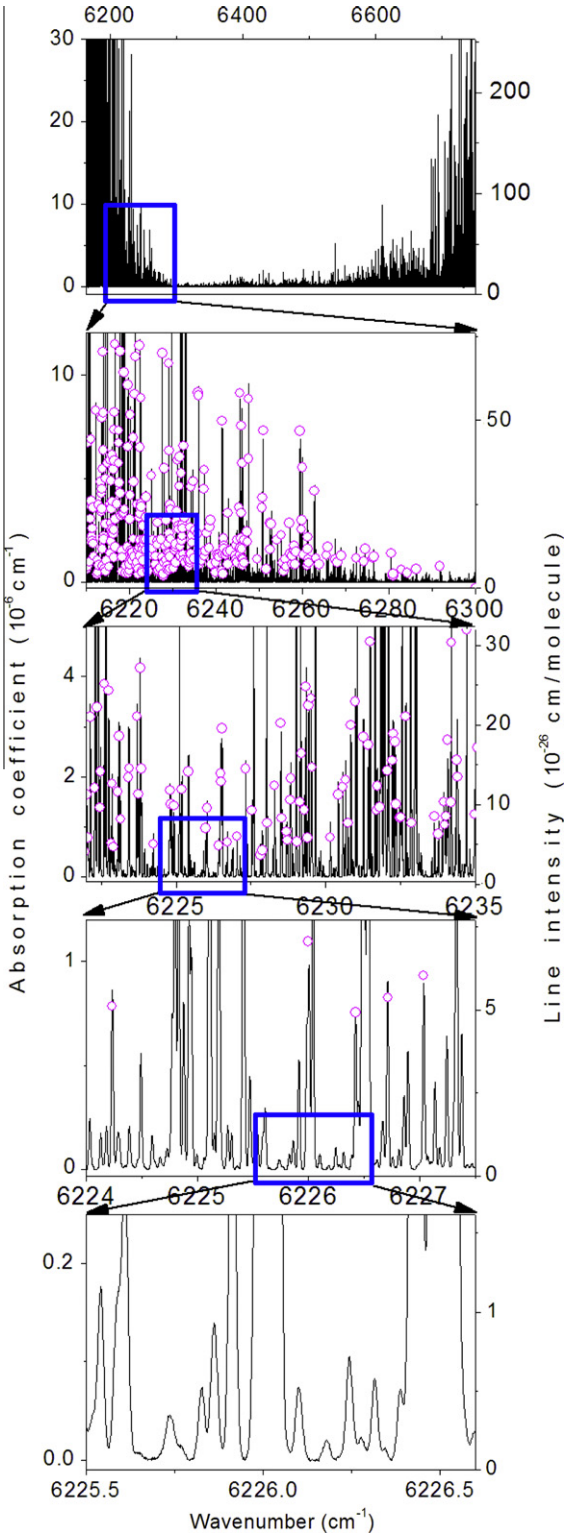

Fig. 2. Four successive enlargements of the CW-CRDS spectrum of methane in the 6165–6750 cm^{-1} region revealing a highly congested structure. The pressure was 1.0 Torr. The open circles mark the lines included in the HITRAN database and correspond to the right hand intensity scale.

the recordings and the impressive congestion of the methane spectrum in the considered transparency window. Absorption coefficients differing by more than four orders of magnitude can be measured from a single CW-CRDS spectrum. Note that, over most of the region, spectral sections free of absorption lines are extremely scarce and the absorption is larger than the noise level.

The line intensity, S_{v_0} (cm/molecule), of a rovibrational transition centred at v_0, was obtained from the integrated absorption coefficient, A_{v_0} (cm^{-2}/molecule):

$$A_{v_0}(T) = \int_{\text{line}} \alpha_v \mathrm{d}v = S_{v_0}(T)N \quad (1)$$

where, v is the wavenumber in cm^{-1}, $\alpha(v)$ is the absorption coefficient in cm^{-1}, and N is the molecular concentration in molecule/cm^3 obtained from the measured pressure and temperature values: $P = NkT$ (k is the Boltzmann constant).

An interactive multi-line fitting program was used to reproduce the spectrum [22]. A Voigt function of the wavenumber was adopted for the line profile as the pressure self broadening has a significant contribution. As isolated lines are exceptions, the first step of the analysis consisted in the manual determination of the spectral sections of overlapping or nearby transitions that could be fitted independently. The local baseline (assumed to be a cubic function of the wavenumber) and the three parameters of each Voigt profile (line center, integrated absorption coefficient, HWHM of the Lorentzian component) were fitted. The HWHM of the Gaussian component was fixed to its theoretical value for $^{12}CH_4$. As a rule, in the case of blended lines or lines with low signal to noise ratios, the Lorentzian HWHM was also constrained to the average value obtained from nearby isolated lines.

It is worth underlining the difficulties of the line profile fitting due to the high density and systematic overlapping of the lines. The average density of lines is 27.7 lines per cm^{-1}. Fig. 3 shows a comparison between the measured and fitted spectra. Some significant differences are noted. They are probably due in part to line

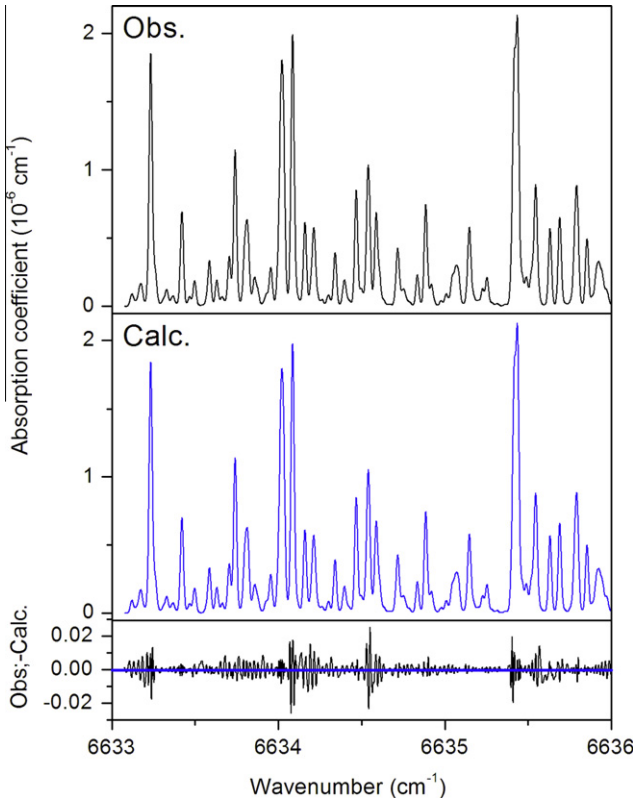

Fig. 3. An example of spectrum reproduction of the CH_4 spectrum illustrating the difficulty of the line by line simulation: in the displayed region, 79 lines had to be simultaneously adjusted to reproduce the observed spectrum. Upper panel: experimental spectrum (P = 9.83 Torr), middle panel: simulated spectrum resulting from the line fitting procedure (a Voigt profile was affected to each line), lower panel: residuals between the simulated and experimental spectra.

mixing effects [23] which were neglected. Some spectral sections required simultaneous profile fitting of up to 100 lines. (This is indeed the case of the fit illustrated in Fig. 3 where 79 lines were simultaneously treated.) In such situations, one must recognize a certain level of subjectivity in the obtained results, the number of components required to reproduce a broad absorption feature being sometimes ambiguous in particular for the weakest lines in the wings of strong lines with intensities larger by three or four orders of magnitude. As a rule, in these ambiguous cases, we preferred to relax the constraints on the Lorentzian width and even on the Gaussian width instead of adding several weak components. These difficulties were encountered because of the sensitivity of the recordings and are mostly limited to the dense background of the weakest lines.

The complete line list provided as Supplementary material was obtained by gathering the line lists corresponding to the different DFB laser diodes. A few H_2O lines present as an impurity in the sample were identified in the high energy part of the investigated region and then deleted. The final CH_4 dataset including the spectroscopic parameters of 6868 lines obtained in Ref. [16] for the 6289–6526 cm^{-1} region, consists in 16,149 entries for the whole 6165–6750 cm^{-1} region (see lower panel of Fig. 1). Their intensity values vary over six orders of magnitude from 1.6×10^{-29} to 2.5×10^{-23} cm/molecule for methane in "natural" abundance at 297 K.

3. Comparison with the HITRAN line list

3.1. Sensitivity

The detailed comparison of our line list with HITRAN08 list provided very interesting information. Fig. 1 shows that CRDS has allowed lowering by more than three orders of magnitude the detectivity threshold in the lowest opacity region near 6400 cm^{-1}. The gain in sensitivity is also illustrated in Fig. 2 where the open circles mark the lines included in the HITRAN database. In order to estimate the relative importance of the newly observed transitions on the absorbance in the region, we have simulated a "low resolution CW-CRDS spectrum" by affecting a 10 cm^{-1} wide (FWHM) normalized Gaussian profile to each line of our list. The resulting absorption coefficient obtained as the product of the obtained simulation by the molecular density (at 1.0 Torr and 296 K) is displayed in Fig. 4 (in logarithmic scale) and compared to a "low resolution HITRAN spectrum" obtained in the same way. The spectra displayed in Fig. 4 shows that the absorption is always larger than 1×10^{-9} cm^{-1}. Of course, the relative impact of the new observations is particularly marked in the 6310–6350 cm^{-1} region where no transitions are listed in HITRAN. Conversely, we note an excellent overall agreement near the low and high energy limits of the investigated region, the transitions newly detected in those regions having a negligible impact compared to the stronger transitions included in HITRAN. We have also included in Fig. 4, the low resolution simulation obtained with the GOSAT line list [9] below 6180 cm^{-1}. The very good agreement between the GOSAT and HITRAN simulations shows that the numerous additional lines with intensities in the 4×10^{-26}–4×10^{-24} cm/molecule range in the GOSAT list add a negligible contribution to the overall absorption.

3.2. Line positions

In order to find automatically the HITRAN lines in coincidence with a CRDS observation, we have used a program which associates a CRDS line and a HITRAN line when both their line centers differ by less than 5×10^{-3} cm^{-1} and their intensities differ by less than 20%. The second condition aims to reduce the number of accidental coincidences. The differences of the line centers displayed in Fig. 5 clearly shows the 1.1×10^{-3} cm^{-1} underestimation of HITRAN values compared to our values. This reflects the above mentioned difference of calibration between the Reims spectra [21] adopted as reference and HITRAN. Of importance, is the observation that the series of lines showing an average (CRDS–HITRAN) difference of -1.8×10^{-3} cm^{-1} between 6320 and 6500 cm^{-1} are due to CH_3D (see Fig. 5). As mentioned above, these CH_3D line positions recently included in the HITRAN database [3] were obtained in Ref. [10]. The relative positions error between the CH_4 and CH_3D transitions pro-

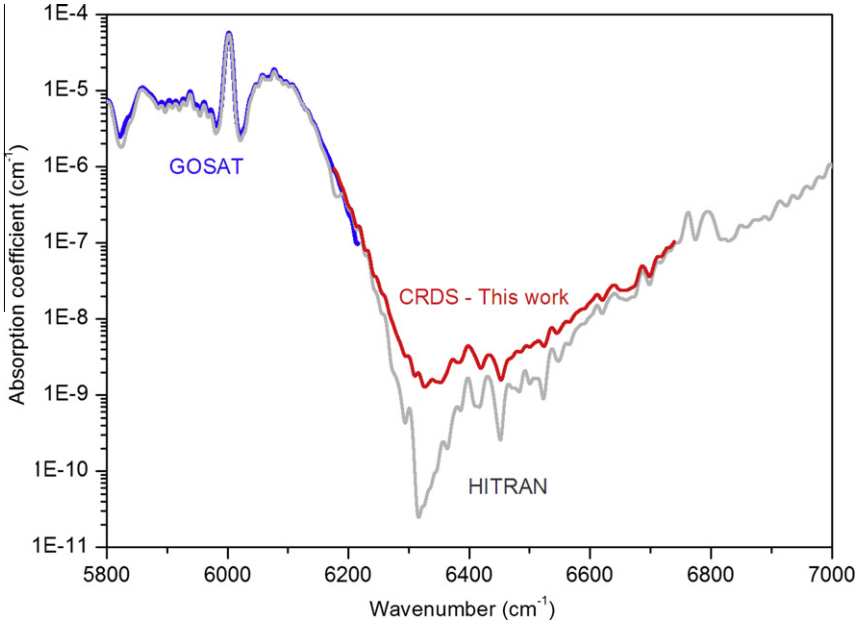

Fig. 4. Comparison of the 'low resolution' absorption spectrum of methane (P = 1.0 Torr) simulated from the CW-CRDS line list (red) and from the HITRAN database (grey). The spectra were obtained by affecting a normalized Gaussian profile (FWHM = 10.0 cm^{-1}) to each line. The GOSAT simulation (blue) displayed below 6200 cm^{-1} is in close coincidence with HITRAN simulation. Note the logarithmic scale adopted for the absorption coefficient. (For interpretation of color mentioned in this figure the reader is referred to the web version of the article.)

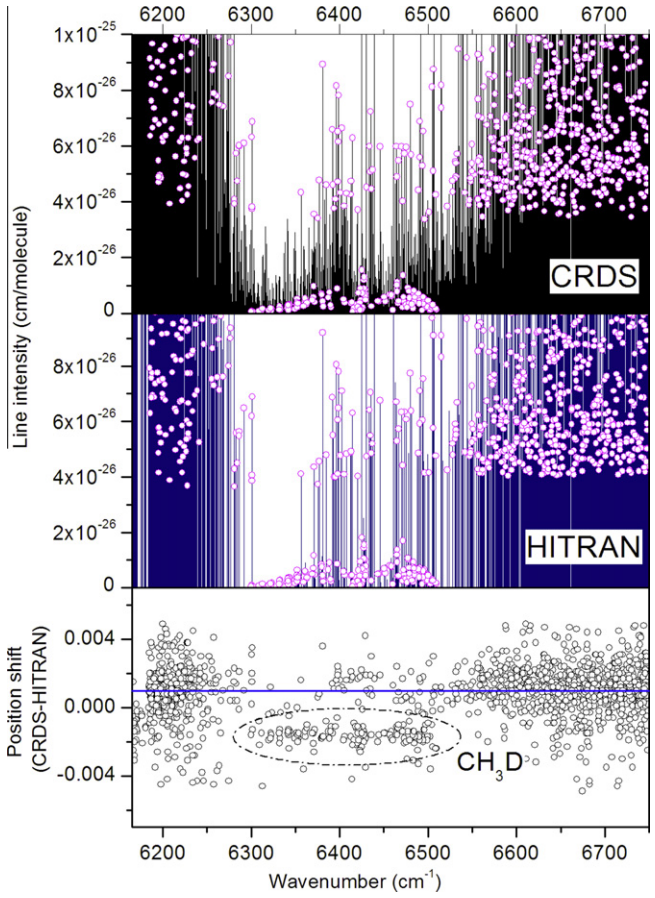

Fig. 5. Comparison of the wavenumber calibration of the CRDS and HITRAN line lists. The stick spectra obtained by CRDS and provided by HITRAN are displayed in the upper and middle panels, respectively. The open circles mark the lines in common in the two dataset (see Text). The lower panel shows the position differences. Compared to HITRAN, the CRDS line positions of CH_4 and CH_3D are on average larger by 1.1×10^{-3} cm^{-1} and smaller than 1.8×10^{-3} cm^{-1}, respectively.

vided in HITRAN is then on the order of 0.003 cm^{-1}. This value agrees well with the claimed uncertainty of the original data used for HITRAN: Brown [7] used CO 2–0 and 3–0 bands as standards to calibrate her CH_4 spectra but quoted 'generic' absolute accuracies of 0.0007 cm^{-1} at 5000 cm^{-1} to 0.0015 cm^{-1} at 7000 cm^{-1} because of the congestion of lines; no calibration standards were used by Lutz et al. [10] which estimated to 0.005 cm^{-1} the absolute accuracy of their CH_3D spectra.

3.3. Line intensities

In order to associate one by one the lines corresponding to the same transition in the CRDS and HITRAN lists, we used the same automatic association program and fixed to 1.0×10^{-3} cm^{-1} the maximum line centers differences (after correction of the 1.1×10^{-3} cm^{-1} calibration shift). The obtained ratios of the CRDS and HITRAN intensities are plotted in Fig. 6 versus the line intensities.

A very good overall agreement is noted for the CH_4 intensity values (average value very close to 1). The large discrepancies observed for some strong lines below 6180 cm^{-1} are due to transitions for which a multiplet structure was used in the CRDS line profile fitting while they appear as single lines in the HITRAN line list. The comparison for the CH_3D intensities evidences a systematic underestimation of the CRDS values, our values being on average 18% smaller than HITRAN values. This discrepancy is significantly higher than the 8% value given by Boussin et al. [11] for the uncertainty of their CH_3D intensities.

Our search of the origin of this disagreement was puzzling.

First, we compared our CH_3D intensity values to those measured from the long path absorption spectrum of methane recorded in Reims and found a very good agreement between these two measurements performed with methane in "natural" abundance.

Second, we checked Boussin's intensity values obtained with CH_3D sample (96.8% purity) by comparison to the FTS spectrum of an enriched CH_3D sample (99% stated purity) recently recorded in Hefei (see Ref. [16] and next section). We found a very good coincidence between these two measurements performed with a highly enriched CH_3D sample.

The conflict between the sets of intensity results retrieved from "natural gas" or enriched CH_3D is only apparent. The CH_3D HITRAN intensity values are scaled according to the CH_3D relative abundance in methane. The 6.15×10^{-4} value adopted in HITRAN for the CH_3D/CH_4 abundance results from the D/H relative abundance (1.5576×10^{-4}) of the Vienna Standard Mean Ocean Water (VSMOW) [24]. This value differs significantly from the CH_3D/CH_4 relative abundance in natural gas as that used for the CRDS and Reims recordings. More precisely, the 18% difference evidenced between the CRDS and HITRAN intensity values of CH_3D coincides exactly to the known δD_{CH4} depletion of CH_3D in natural gas compared to the VSMOW value (see Fig. 1 of Ref. [25], for instance).

As mentioned in the Section 1 (Fig. 1), Deng et al. have recorded the methane spectrum in the 6607–6625 cm^{-1} section by direct absorption spectroscopy using a DFB laser source of the same type as used for our CRDS recordings, which was coupled to a White cell with a maximum path length of 973 m [17]. In the studied 18 cm^{-1} wide interval, 288 lines were measured with intensities down to 1.4×10^{-27} cm/molecule which improved the HITRAN line list (67 transitions above 4×10^{-26} cm/molecule). For comparison, our line list provides 468 lines in the same region. The line by line comparison of the intensity ratios presented in Fig. 7 shows a reasonable agreement.

4. Identification of the CH_3D transitions

Considering the variation of the CH_3D/CH_4 relative abundance in the various sources of methane on Earth [25] and in planetary atmospheres [15], the discrimination of the CH_3D and CH_4 transitions is necessary to be able to scale their relative intensities according to the relative abundance value.

Practically all the $3\nu_2$ transitions of CH_3D included in the HITRAN list could be identified in our line list between 6300 and 6520 cm^{-1} [16]. The HITRAN list for CH_3D is limited to the transitions of the $3\nu_2$ transitions with intensity larger than 1.4×10^{-28} cm/molecule, which is above the sensitivity of our spectra (see Fig. 1). In order to identify further CH_3D transitions in our line list, the FTS spectrum of CH_3D was recorded at USTC (Hefei, China) [16]. The enriched CH_3D methane sample had a stated purity of 99%. The recordings were performed with unapodized resolution of 0.015 cm^{-1} and several absorption path lengths (15, 33 and 51 m) and pressure values (4.17 and 19.92 Torr) were used.

This FTS spectrum revealed a high number of lines not included in HITRAN (see Fig. 8 of Ref. [16]). They were identified in the CRDS spectra of methane using both positions and intensities as criteria (see Fig. 8 for instance). Obviously, a fraction of the CH_3D transitions were found superimposed with CH_4 transitions. In the line list attached as Supplementary material, the CH_3D transitions are indicated together with the CH_4 transitions which are believed to be strongly blended with CH_3D lines. Finally, among the 16,149 CRDS transitions of methane, 1385 were attributed to CH_3D and

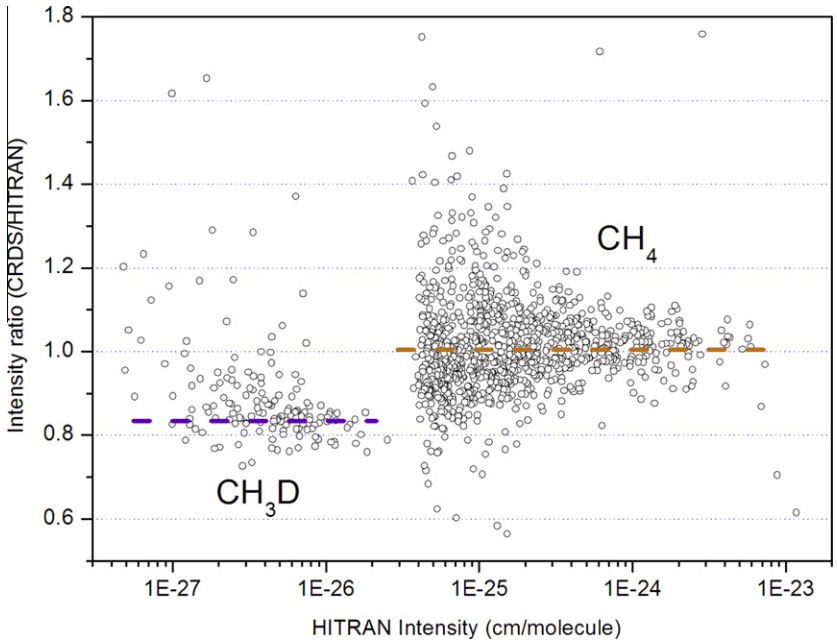

Fig. 6. Variation of the ratios of the CRDS and HITRAN line intensities of methane transitions in the 6165–6750 cm^{-1} region versus the HITRAN intensity values. The lines with intensities smaller than 3×10^{-26} cm/molecule are due to CH_3D. The 0.82 average value of the CH_3D ratios reflects the 18% depletion of CH_3D in natural gas compared to the HITRAN relative abundance value (see Text). The large discrepancies observed for some of the strongest lines are due to transitions below 6180 cm^{-1} for which a multiplet structure was used in the CRDS line profile fitting while they appear as single lines in the HITRAN line list.

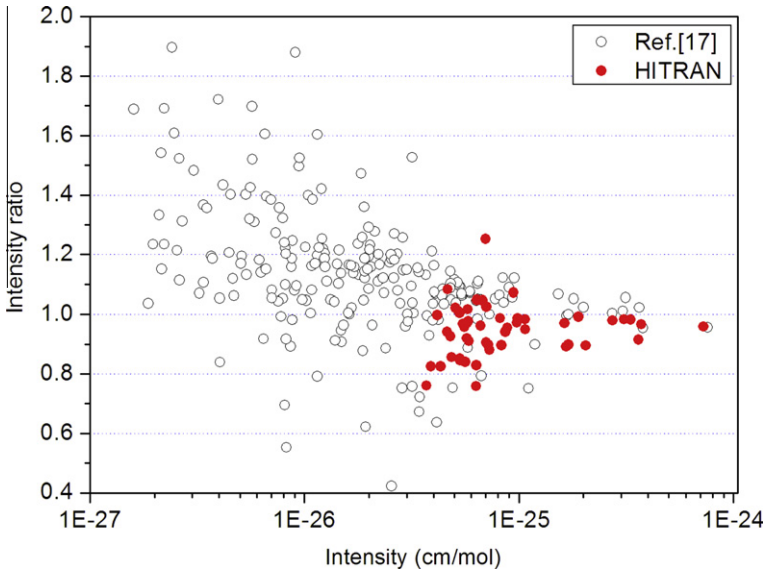

Fig. 7. Ratios of the CRDS intensities with the intensity values of Ref. [17] (open circles) and HITRAN values (full circles) for the 6607 and 6625 cm^{-1} region.

1115 transitions are believed to have an important contribution of both isotopologues. Let us underline that the CH_3D intensities in our list correspond to a CH_3D/CH_4 relative abundance which is about 18% smaller than HITRAN value.

In order to further quantify the CH_3D contribution to the methane absorption in the region, we present on Fig. 9 a comparison of the low resolution simulation of the absorption spectra of methane and CH_3D in "natural" abundance. The methane spectrum was calculated from the CRDS line list as described in Section 3. The CH_3D absorption was simulated by convolution with a 10 cm^{-1} wide (FWHM) Gaussian function of the FTS absorbance normalized by the pressure (in Torr) and the absorption pathlength (in cm); the obtained result being multiplied by the HITRAN value of the CH_3D abundance. For comparison, the low resolution simulation of the $3\nu_2$ band of CH_3D as provided in HITRAN is also included in Fig. 9. The obtained curves show that the CH_3D relative contribution is negligible outside the 6260–6530 cm^{-1} interval and that it represents about 30% of the total absorption near the Q branch of the $3\nu_2$ band at 6430 cm^{-1} and in the lowest opacity region near 6320 cm^{-1}. The lack of completeness of the HITRAN database in this last region is then the most prejudicial.

In absence of a high sensitivity spectrum of the $^{13}CH_4$ isotopologue, the $^{12}CH_4$ and $^{13}CH_4$ transitions could not be discriminated. Nevertheless, the $^{13}C/^{12}C$ isotopic substitution leads to much smal-

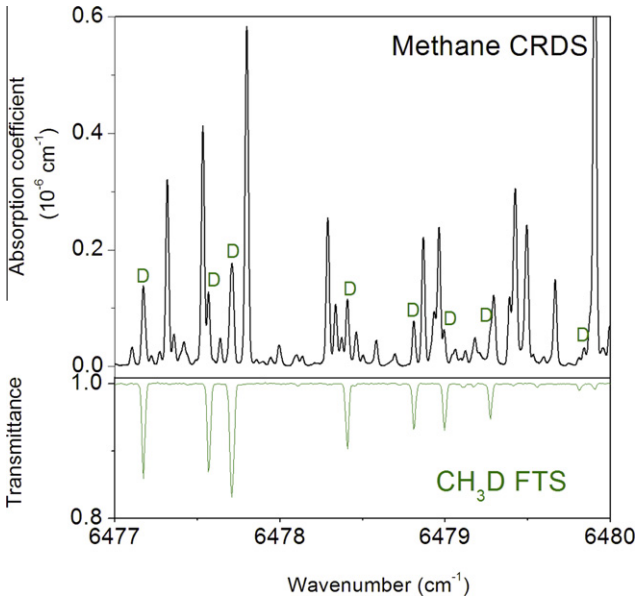

Fig. 8. Identification of the CH_3D transitions (marked with "D") contributing to the methane absorption near 6296 cm^{-1}. Upper panel: CW-CRDS spectrum of methane (P = 1.0 Torr). Lower panel: FTS spectrum of CH_3D (99% stated purity) recorded with a sample pressure of 4.17 Torr and an absorption pathlength of 15 m.

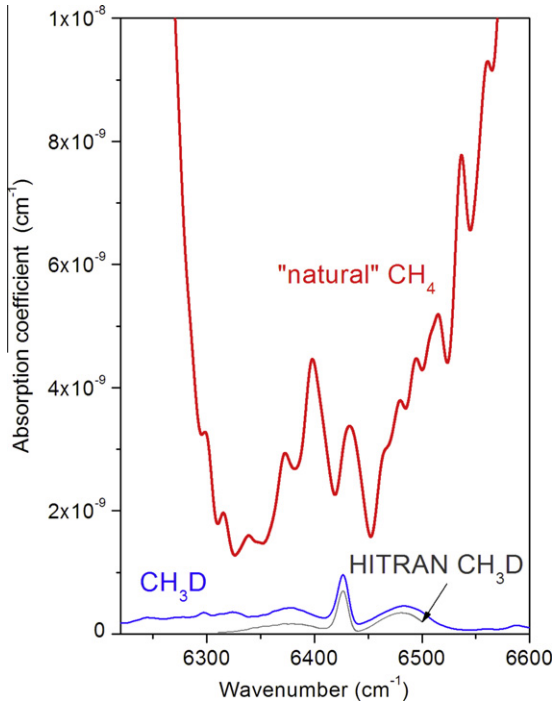

Fig. 9. Contribution of the CH_3D isotopologue to the absorption spectrum of methane between 6220 and 6600 cm^{-1} (P = 1.0 Torr). The 'low resolution' spectrum of methane was simulated from the CW-CRDS line list (red) while the CH_3D simulation (blue) is a convolution of the FTS spectrum of CH_3D with a normalized Gaussian profile (FWHM = 10.0 cm^{-1}) scaled according to the HITRAN abundance. The 'low resolution' simulation of the $3\nu_2$ band of CH_3D as provided in HITRAN is also displayed. (For interpretation of color mentioned in this figure the reader is referred to the web version of the article.)

ler isotopic shifts of the vibrational bands [26] compared to the D/H substitution. In consequence, all over the transparency window, the $^{13}CH_4$ relative contribution to the absorbance is expected to be on the same order of magnitude than the 1.1% relative abundance of this isotopologue.

5. Conclusion

We have completed the spectral coverage of the absorption spectrum of methane in the 1.58 μm transparency window by high sensitivity Cavity Ring Down Spectroscopy at room temperature. The achieved sensitivity ($\alpha_{min} \sim 3 \times 10^{-10}$ cm^{-1}) has allowed measuring line intensities as weak as 1.6×10^{-29} cm/molecule i.e. three orders of magnitude below the intensity cut off of the HITRAN line list. Overall, the line list attached as Supplementary material provides the positions and strengths of 16,149 transitions between 6165 and 6750 cm^{-1}. The significance of these observations is illustrated by Fig. 1 and Table 1 which presents the overall comparison with previous works. On the basis of a FTS spectrum of CH_3D, the CH_3D transitions could be discriminated. The apparent discrepancy between the CH_3D/CH_4 relative intensities measured in our CRDS spectra of methane and provided in HITRAN was explained by the difference between the CH_3D/CH_4 abundance ratio in natural gas and the VSMOW relative abundance adopted in HITRAN. Interestingly, the CH_3D abundance in our sample (about 5×10^{-4}) is very close to the CH_3D/CH_4 abundance on Titan [12,13,27,28].

The relative contribution of the CH_3D isotopologue estimated by simulation of the CH_3D and methane spectra at low resolution (10 cm^{-1} FWHM) has shown that, in spite of its very small relative abundance, the CH_3D absorption contributes to up to 30% of the absorbance in the region. Considering the large variation of the CH_3D/CH_4 ratios in the different planetary atmospheres [15], the accurate calculation of the transmission in the considered transparency window requires scaling the CH_3D intensities according to the CH_3D/CH_4 relative abundance of the considered medium. For instance, the CH_3D relative concentrations on Jupiter and Saturn being about 10 times less than in the Earth atmosphere [15], the CH_3D contribution to the absorption near 1.58 μm will be marginal on these planets.

Considering the large variety of temperature conditions, planetary applications require also the knowledge of the temperature dependence of the methane spectra. Indeed, the methane spectrum at both high and low resolution (for instance, the overall shape of the 1.58 μm transparency window), is highly sensitive to the temperature [16,29]. We have recently used the "two temperature method" to derive the lower state energy necessary to compute the Boltzmann factors which rule the temperature dependence of the line intensities. From the ratio of the line intensities measured at room temperature and at liquid nitrogen temperature, the low energy levels of the transitions in common in the two spectra were obtained. The "two temperature method" is a robust and reliable method which was successfully applied to the high absorbing regions surrounding the presently studied transparency window at 1.58 μm [29–34]. In these regions, the spectra at 81 K were obtained by differential absorption spectroscopy using a specifically designed cryogenic cell and a series of several tens DFB diode lasers [29]. This experimental approach provided a sufficient sensitivity ($\alpha_{min} \sim 10^{-6}$ cm^{-1}) in the high energy part of the tetradecad (5850–6180 cm^{-1}) [29–31] and in the icosad region (6700–7700 cm^{-1}) [33,34]. In the 1.58 μm transparency window corresponding to the 6180–6750 cm^{-1} gap, a much higher sensitivity is required. We have recently been able to combine the CW-CRDS technique with the same cryogenic cell [35]. The sensitivity achieved by CW-CRDS at 80 K and room temperature are equivalent [35] ($\alpha_{min} \sim 3 \times 10^{-10}$ cm^{-1}). In Ref. [16], the "two temperature method" has been applied to the CRDS spectra in the region of the the $3\nu_2$ band of CH_3D (6289–6526 cm^{-1}). After the present

Table 1
Summary and statistics of the most relevant investigations of the methane spectrum in the 1.58 μm transparency window.

		Range (cm^{-1})	Number of lines in the 6165–6750 cm^{-1} region	Minimum intensity (cm/molecule)
This work		6165–6750	16149[a]	$\sim 3 \times 10^{-29}$
HITRAN08	CH_4 from Brown [7]	6180–9200	1875	4×10^{-26}
	CH_3D: from Lutz et al. [10] and Boussin et al. [11]	6300–6510	251	1.4×10^{-28}[b]
Deng et al. [17]		6607–6625	288	$\sim 2 \times 10^{-27}$

[a] Including 6868 transitions reported in Ref. [16].
[b] This value takes into account the CH_3D/CH_4 abundance (6.15×10^{-4}) value adopted in HITRAN.

completion of the room temperature line list over the whole transparency window, the next step will be the construction of a similar line list at 80 K in order to determine the lower state energy. By gathering, the results obtained in Refs. [16,31,33], we hope to provide in a near future a line list allowing accounting for the temperature dependence of the methane absorption over the whole 1.26–1.70 μm range.

Acknowledgements

This work is part of the ANR project "CH4@Titan" (ref: BLAN08-2_321467) which is a joint effort among four French laboratories (ICB-Dijon, GSMA-Reims, LSP-Grenoble and LESIA-Meudon) to adequately model the methane opacity. We would like to thank E. Kerstel (University of Groningen), J. Chappelaz and J. Savarino (LGGE, Grenoble) for valuable discussions relative to the CH_3D/CH_4 abundance. We thank the GSMA group (University of Reims) for providing us with their long path absorption spectrum of methane which was used to refine the wavenumber calibration of our spectra. The support of the Groupement de Recherche International SAMIA between CNRS (France), RFBR (Russia) and CAS (China) is acknowledged.

Appendix A. Supplementary data

Supplementary data associated with this article can be found, in the online version, at doi:10.1016/j.chemphys.2010.05.011.

References

[1] V. Boudon, M. Rey, M. Loëte, J. Quant. Spectrosc. Radiat. Transfer 98 (2006) 394.
[2] J. Bowman, T. Carrington, H.-D. Meyer, Mol. Phys. 106 (2008) 2145.
[3] L.S. Rothman, I.E. Gordon, A. Barbe, D.C. Benner, P.F. Bernath, et al., J. Quant. Spectrosc. Radiat. Transfer 110 (2009) 533.
[4] J.S. Margolis, Appl. Opt. 27 (1988) 4038.
[5] J.S. Margolis, Appl. Opt. 29 (1990) 2295.
[6] C. Frankenberg, T. Warneke, A. Butz, I. Aben, F. Hase, P. Spietz, L.R. Brown, Atmos. Chem. Phys. 8 (2008) 5061.
[7] L.R. Brown, J. Quant. Spectrosc. Radiat. Transfer 96 (2005) 251.
[8] Available from: <http://gosat.nies.go.jp>.
[9] A.V. Nikitin, O.M. Lyulin, S.N. Mikhailenko, V.I. Perevalov, N.N. Filippov, I.M. Grigoriev, I. Morino, T. Yokota, R. Kumazawa, T. Watanabe, J. Quant. Spectrosc. Radiat. Transfer (accepted for publication), doi:10.1016/j.jqsrt.2010.05.010.
[10] B.L. Lutz, C. de Bergh, J.-P. Maillard, Astrophys. J. 273 (1983) 397.
[11] C. Boussin, B.L. Lutz, C. de Bergh, A. Hamdouni, J. Quant. Spectrosc. Radiat. Transfer 60 (1998) 501.
[12] P.F. Penteado, C.A. Griffith, T.K. Greathouse, C. de Bergh, Astrophys. J. 629 (2005) L53.
[13] P.F. Penteado, C.A. Griffith, Icarus 206 (2010) 345.
[14] C. de Bergh, B.L. Lutz, T. Owen, J. Chauville, Astrophys. J. 329 (1988) 951.
[15] C. de Bergh, B.L. Lutz, T. Owen, J.-P. Maillard, Astrophys. J. 355 (1990) 661.
[16] L. Wang, S. Kassi, A.W. Liu, S.M. Hu, A. Campargue, J. Mol. Spectrosc. 261 (2010) 41.
[17] L.-H. Deng, X.-M. Gao, Z.-S. Cao, W.-D. Chen, W.-J. Zhang, Z.-B. Gong, J. Quant. Spectrosc. Radiat. Transfer 103 (2007) 402.
[18] A.W. Liu, S. Kassi, A. Campargue, Chem. Phys. Lett. 447 (2007) 16.
[19] J. Morville, D. Romanini, A.A. Kachanov, M. Chenevier, Appl. Phys. D78 (2004) 465.
[20] B.V. Perevalov, S. Kassi, D. Romanini, V.I. Perevalov, S.A. Tashkun, A. Campargue, J. Mol. Spectrosc. 238 (2006) 241.
[21] A.V. Nikitin, X. Thomas, L. Regalia, L. Daumont, P. von der Heyden, Vl.G. Tyuterev, Le Wang, S. Kassi, A. Campargue, (submitted for publication).
[22] L. Daumont, J. Vander Auwera, J.-L. Teffo, V.I. Perevalov, S.A. Tashkun, J. Mol. Spectrosc. 208 (2001) 281.
[23] H. Tran, J.-M. Hartmann, G. Toon, L.R. Brown, C. Frankenberg, T. Warneke, P. Spietz, F. Hase, J. Quant. Spectrosc. Radiat. Transfer 111 (2010) 1344.
[24] P. De Bievre, N.E. Holden, I.L. Barnes, J. Phys. Chem. Ref. Data 13 (1984) 809.
[25] T. Sowers, Science 838 (2006) 311.
[26] A.V. Nikitin, S. Mikhailenko, I. Morino, T. Yokota, R. Kumazawa, T. Watanabe, J. Quant. Spectrosc. Radiat. Transfer 110 (2009) 964.
[27] B. Bézard, C.A. Nixon, I. Kleiner, D.E. Jennings, Icarus 191 (2007) 397.
[28] A. Coustenis, R. Achterberg, B. Conrath, et al., Icarus 189 (2007) 35.
[29] S. Kassi, B. Gao, D. Romanini, A. Campargue, Phys. Chem. Chem. Phys. 10 (2008) 4410.
[30] B. Gao, S. Kassi, A. Campargue, J. Mol. Spectrosc. 253 (2009) 55.
[31] L. Wang, S. Kassi, A. Campargue, J. Quant. Spectrosc. Radiat. Transfer 111 (2010) 1130.
[32] E. Sciamma-O'Brien, S. Kassi, B. Gao, A. Campargue, J. Quant. Spectrosc. Radiat. Transfer 110 (2009) 951.
[33] A. Campargue, L. Wang, S. Kassi, M. Mašát, O. Votava, J. Quant. Spectrosc. Radiat. Transfer 111 (2010) 1130.
[34] O. Votava, M. Mašát, P. Pracna, S. Kassi, A. Campargue, Phys. Chem. Chem. Phys. 12 (2010) 3145.
[35] S. Kassi, D. Romanini, A. Campargue, Chem. Phys. Lett. 477 (2009) 17.